

# Compass Gait Control with Switched Reference Partial Feedback Linearization\*

Luís Filipe Rossi<sup>1</sup>, Pierluigi Nichilo<sup>1,2</sup> and A. Forner-Cordero<sup>1</sup>, *IEEE Member*

**Abstract**—Passive Dynamic Walking overcomes elegantly several drawbacks of the high gain position control approach to generate bipedal gait of robots. In this scenario the Limit Cycle Walking concept leads to the generation of high energetically efficient gait. The goal of this paper is to demonstrate how the implementation of an ex-novo controller - based on switched reference partial feedback linearization - can increase the basin of attraction of a Limit Walking Cycle. The simulation has been performed on a compass gait model. The controller simulation and the mechanical model description have been defined through a range of initial conditions for the state variables. The results demonstrated that the controller was able to increase the basin of attraction of the compass gait model with respect to the passive system. The novel controller has a low computational load, which makes it a perfect candidate for the implementation on real prototypes.

## I. INTRODUCTION

Bipedal robot performance improved a lot in the last decades thanks to the progress in both the robot hardware components production (actuators, sensors and batteries) and the development of new biped stability criteria, some of them emerging from passive dynamic walking studies [1]. Nevertheless, the massive execution of several pre-programmed tasks in real world applications presents many issues. It means that the ability to perform very robust and reliable steps - thus, a good resistance to perturbations - might be pursued only refining the gait control tools.

Many biped robots (i.e. ASIMO [2] and HRP-4C [3]) perform a stable gait through the implementation of the Zero Moment Point method [4]. It allows a robot to maintain its balance by keeping its Zero Moment Point within set boundaries at any given point in the robot walking gait. They are able to walk upright without falling over, moving much slower and less naturally than a human. Moreover, a high gain position control is required, which significantly downs the energetic efficiency of the system.

The Passive Dynamic Walking [1] theory solves this problem taking advantage of the biped dynamics. Theoretically, the Limit Cycle Walking [5] is a periodic sequence of steps: an exact repetition of a closed trajectory in state space, where each of the walker two feet are alternately forwarded. The walking motion starts by launching the robot with such initial values for the leg angles and velocities, that at the end of

that step (the beginning of a new one) is nearly identical to the previous starting conditions [6]. The set of the state variables values allowing for a stable gait is known as **the basin of attraction** of the system.

Several recent works have adopted different control strategies to increase the existing basin of attraction of Limit Cycle Walkers leading to an improved robustness to perturbations. Spong [7] developed a potential energy shaping controller which leads to a system invariant under slopes changes. Iida [8] demonstrated that an open-loop sinusoidal oscillation at the hip joint of a compass gait model can lead to an increase of the basin of attraction, while Kochuvila [9] presented and compared a feedback linearization controller with a partial feedback linearization controller.

This paper presents the application of a partial feedback linearization controller to the passive dynamic walker, in order to improve its stability and disturbance rejection. The novelty of this work consists of the application of a switching algorithm: once both the legs have been simultaneously affected by disturbances, it alternatively recovers the most perturbed leg.

The rest of the paper is organized as follows: Section II provides a physical description of the compass gait model, details the dynamic equations and states the assumptions taken during the analysis. Section III describes the control algorithm. Section IV presents preliminary simulations and results; a list of future developments of this work is provided as well. Finally, section V presents the conclusions.

## II. METHODS

### A. Mechanical Model

The model used to study Passive Dynamic Walking is the compass gait walking model. Due to its simplistic nature, it has been intensively studied from the mechanical, dynamic and control perspective. Therefore, it will be used for testing the proposed concept of this work. The model followed (illustrated in Fig. 1) was adapted from [10].

$$M(\theta)\ddot{\theta} + N(\theta, \dot{\theta})\dot{\theta} + G(\theta) = Bu \quad (1)$$

Equation (1) describes the system dynamics where  $u = \begin{pmatrix} u_H \\ u_a \end{pmatrix}$ ,  $u_H$  being the hip joint torque and  $u_a$  the ankle joint torque,  $\theta = \begin{pmatrix} \theta_{ns} \\ \theta_s \end{pmatrix}$  and:

\*This work was supported by CNPq

<sup>1</sup>Luís Filipe Rossi and Arturo Forner Cordero are with the University of São Paulo, São Paulo, Brazil corresponding author: aforner@usp.br

<sup>2</sup>Pierluigi Nichilo with the Mechanical Engineering Department, Politecnico di Torino, Torino, Italy pierluigi.nichilo@studenti.polito.it

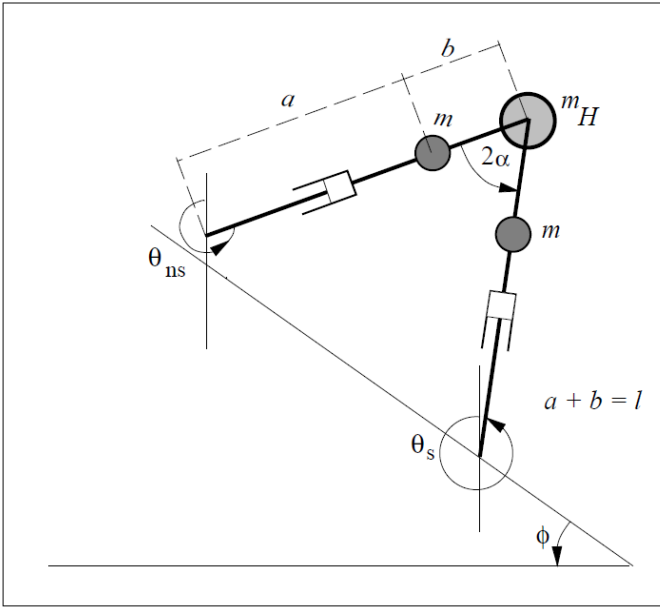


Fig. 1. Compass Gait Model [10]

$$M(\theta) = \begin{pmatrix} M_{11} & M_{12} \\ M_{21} & M_{22} \end{pmatrix} \quad (2a)$$

$$M_{11} = mb^2 \quad (2b)$$

$$M_{12} = -mlb \cos(\theta_s - \theta_{ns}) \quad (2c)$$

$$M_{21} = -mlb \cos(\theta_s - \theta_{ns}) \quad (2d)$$

$$M_{22} = (m_H + m)l^2 + ma^2 \quad (2e)$$

$$N(\theta, \dot{\theta}) = \begin{pmatrix} N_{11} & N_{12} \\ N_{21} & N_{22} \end{pmatrix} \quad (3a)$$

$$N_{11} = 0 \quad (3b)$$

$$N_{12} = mlb\dot{\theta}_s \sin(\theta_s - \theta_{ns}) \quad (3c)$$

$$N_{21} = -mlb\dot{\theta}_{ns} \sin(\theta_s - \theta_{ns}) \quad (3d)$$

$$N_{22} = 0 \quad (3e)$$

$$G(\theta) = \begin{pmatrix} G_1 \\ G_2 \end{pmatrix} \quad (4a)$$

$$G_1 = mgb \sin(\theta_{ns}) \quad (4b)$$

$$G_2 = -(m_H l + ma + ml)g \sin(\theta_s) \quad (4c)$$

$$B = \begin{pmatrix} -1 & 1 \\ 1 & 0 \end{pmatrix} \quad (5)$$

Rearranging the above expression in a more compact form, it gives:

$$N(\theta, \dot{\theta})\dot{\theta} + G(\theta) = \begin{pmatrix} C_1 \\ C_2 \end{pmatrix} \quad (6)$$

The assumptions at foot contact are: instantaneous change in angular velocity and perfect inelastic collision. The resulting loss of kinetic energy is restored by gravity, since the ramp is tilted, therefore, conserving the total angular momentum.

Considering the same impact model as [10], and that the impact takes place at time  $t = T$  and that  $2\alpha = \theta_s(T) - \theta_{ns}(T)$ , the following impact model is defined:

$$\dot{\theta}(T^+) = I(\theta(T))\dot{\theta}(T^-) \quad (7)$$

$$I(\theta(T)) = Q(\alpha)^{-1}P(\alpha) \quad (8)$$

$$P(\alpha) = \begin{pmatrix} (m_H l + 2m(m-b))l \cos(2\alpha) & -mab \\ -mab & 0 \end{pmatrix} \quad (9)$$

$$Q(\alpha) = \begin{pmatrix} mb^2 - mbl \cos(2\alpha) & (ml^2 + ma^2 + m_H l^2) \\ -mab & 0 \end{pmatrix} \quad (10)$$

In the proposed work  $u_a$  is considered to be zero all the time and the parameters stated at Table I have been used during the simulations.

TABLE I  
MODEL ATTRIBUTES

Attribute	Value
$m_H$	10 Kg
$m$	5 Kg
$a$	0.5 m
$b$	0.5 m
$g$	9.8 m/s <sup>2</sup>
$\phi$	0.0524 rad

## B. Control

In order to reach a limit cycle, all the controlled states must be led to a proper condition. As the proposed model is underactuated, it is not possible to use feedback linearization. Nevertheless, partial feedback linearization can be used [9]. Still, as we have a single control input, just  $\theta_s$  or  $\theta_{ns}$  can be tracked every time. Therefore, a switched reference control is used: two control laws are created, one for tracking the pair  $\theta_s/\dot{\theta}_s$  and a second one for tracking the pair  $\theta_{ns}/\dot{\theta}_{ns}$ . Finally, a switching law is created in order to instantaneously select the control law to be used.

1) *Control Laws:* Expanding (1) we have:

$$M_{11}\ddot{\theta}_{ns} + M_{12}\ddot{\theta}_s + C_1 = -u_H \quad (11)$$

$$M_{21}\ddot{\theta}_{ns} + M_{22}\ddot{\theta}_s + C_2 = u_H \quad (12)$$

Isolating  $\ddot{\theta}_{ns}$  and  $\ddot{\theta}_s$  at (11) we get:

$$\ddot{\theta}_s = -\frac{1}{M_{12}}(u_H + M_{11}\ddot{\theta}_{ns} + C_1) \quad (13)$$

$$\ddot{\theta}_{ns} = -\frac{1}{M_{11}}(u_H + M_{12}\ddot{\theta}_s + C_1) \quad (14)$$

Considering  $\theta_s^{tar}$ ,  $\theta_{ns}^{tar}$ ,  $\dot{\theta}_s^{tar}$  and  $\dot{\theta}_{ns}^{tar}$  the target reference values at a certain time we have the following control laws:

$$\mathcal{V}_s = \ddot{\theta}_s^{tar} - K_0(\theta_s - \theta_s^{tar}) - K_1(\dot{\theta}_s - \dot{\theta}_s^{tar}) \quad (15)$$

$$\mathcal{V}_{ns} = \ddot{\theta}_{ns}^{tar} - K_0(\theta_{ns} - \theta_{ns}^{tar}) - K_1(\dot{\theta}_{ns} - \dot{\theta}_{ns}^{tar}) \quad (16)$$

Substituting (13), (14), (15) and (16) at (12) we have the following:

$$u_H^s = \frac{M_{21}(-\frac{1}{M_{11}}(M_{12}\mathcal{V}_s + C_1)) + M_{22}\mathcal{V}_s + C_2}{1 + \frac{M_{21}}{M_{11}}} \quad (17)$$

$$u_H^{ns} = \frac{M_{21}\mathcal{V}_{ns} + M_{22}(-\frac{1}{M_{12}}(M_{11}\mathcal{V}_{ns} + C_1)) + C_2}{1 + \frac{M_{22}}{M_{12}}} \quad (18)$$

The equations (17) and (18) are the resultant of the partial feedback linearization considered in respect to  $\theta_s$  and  $\theta_{ns}$  respectively.

In order to find  $\theta_s^{tar}$ ,  $\theta_{ns}^{tar}$ ,  $\dot{\theta}_s^{tar}$  and  $\dot{\theta}_{ns}^{tar}$  the described model was simulated with no torque input with the initial conditions as highlighted in the Table II.

TABLE II  
INITIAL VALUES

State	Value
$\theta_{ns}$	0 rad
$\theta_s$	0 rad
$\dot{\theta}_{ns}$	2 rad/s
$\dot{\theta}_s$	-0.4 rad/s

Fig. 2(a) and Fig. 2(b) illustrates the acquired desired trajectory.

2) *Switching Law*: The switching law is the key to use a control algorithm that is able to track the limit cycle successfully. The basic idea implemented in this work is to treat  $\theta_s$  as the base point to find all other states values, as the stance leg is more complicated to control. If it is out of the range of the passive limit cycle,  $\theta_s^{tar}$  is chosen as the closest valid value and  $u_H^s$  is applied to  $u_H$ . Otherwise, the actual  $\theta_s$  is treated as the  $\theta_s^{tar}$  and both the switching law described by (19), (20) and the Algorithm 1 are applied.

$$E_{ns} = K_0 * (\theta_{ns}^{tar} - \theta_{ns})^2 + K_1 * (\dot{\theta}_{ns}^{tar} - \dot{\theta}_{ns})^2 \quad (19)$$

$$E_s = K_0 * (\theta_s^{tar} - \theta_s)^2 + K_1 * (\dot{\theta}_s^{tar} - \dot{\theta}_s)^2 \quad (20)$$

---

**Algorithm 1** Switching Law

---

**if**  $E_s > E_{ns}$  **then**

$u_H \leftarrow u_H^s$

**else**

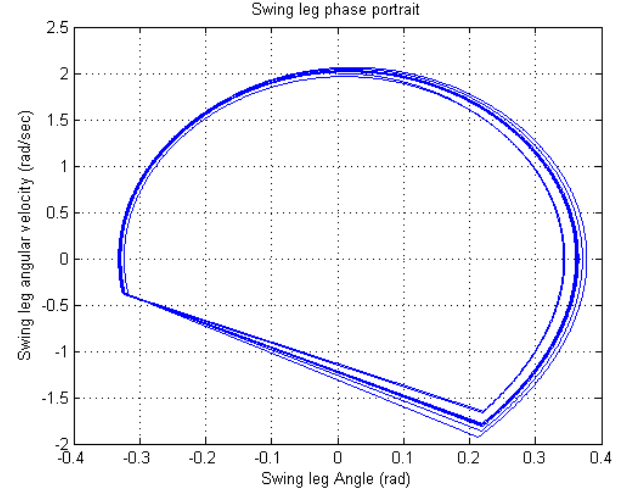
$u_H \leftarrow u_H^{ns}$

**end if**

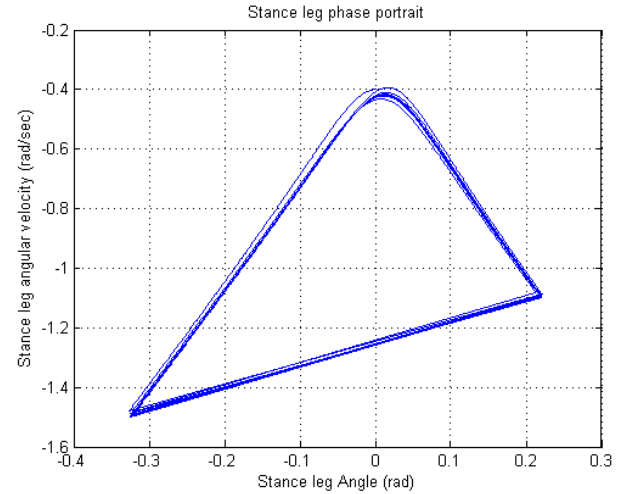
---

The quadratic errors of the position and velocity are calculated for  $\theta_{ns}$  and  $\theta_s$ , thanks to the linear controller gains. If  $E_s$  is bigger than  $E_{ns}$ ,  $u_H^s$  is applied to  $u_H$  and if the opposite is true  $u_H^{ns}$  is applied to  $u_H$ . Finally, wherever the controller is able to reach the passive basin of attraction

of the system, it should stop acting, leaving the system to its natural dynamic. However, it must be noted that finding the real basin of attraction is not a simple task, thus a simplified model was used. Table III shows the ranges of the values of the basin of attraction. If all states values belong to these ranges, simultaneously compared to the reference, the system is considered within the basin of attraction.



(a) Swing Leg



(b) Stance Leg

Fig. 2. Desired Trajectory

TABLE III  
BASIN OF ATTRACTION MODEL

State	Value
$\theta_{ns}$	0.02 rad
$\theta_s$	0.02 rad
$\dot{\theta}_{ns}$	0.21 rad/s
$\dot{\theta}_s$	0.21 rad/s

### C. Simulations

The simulations have been performed with MATLAB (The Mathworks); the ODE45 solver has been used to integrate the differential equations. The set of four coordinates defining the state conditions of the motion has been varied as described in the Table IV: approximately 290,000 simulation cases have been performed, in order to clearly define whether or not the partial feedback linearization control was able to increase the basin of attraction of the passive walker with no control.

TABLE IV  
SIMULATED INTERVAL

State	Initial	Final	Step
$\theta_{ns}$	-0.7 rad	0.7 rad	0.05 rad
$\theta_s$	-0.7 rad	0.7 rad	0.05 rad
$\dot{\theta}_{ns}$	-5 rad/s	2.5 rad/s	0.4 rad/s
$\dot{\theta}_s$	-3 rad/s	0.2 rad/s	0.18 rad/s

### III. RESULTS AND DISCUSSIONS

A quantitative analysis revealed that the passive system has 3,883 different simulated initial conditions determining a stable gait, against the 12,043 assuring the stability of the partial feedback controlled one. That means it was observed an increase of the basin of attraction area of approximately 210.1%. This result is definitively proving the effectiveness of the proposed control approach. It is important to mention that, although the number of stable initial configurations is very small compared to the total set that was tested, there are several configurations that, with the torque limit of the model, are dynamically impossible to be recovered.

The relatively high number of variables (four) defining the state condition of the biped is such that all the information cannot be included in a single graph. A valid alternative has been conceived by plotting data in 3D graphs. In essence, the x and y axis plot respectively the angle and the angular velocity of the leg under analysis, while the z coordinate - Basin of Attraction Density Function - represents the width of the interval (of either the angle or the angular velocity, depending on the chosen parameter) in which the system converges for that given pair of values given on the x-y plane.

By varying all the available kinematics parameters under analysis (the reference leg, either for the x-y or the z coordinate, as well as the variable represented on the z axis) and plotting the data as explained above, a total of 8 graphs results. The first remarkable information inferred from the graph is the increase of the basin of attraction of the controlled with respect to the passive system. This transition is such that, even though the number of angle-angular velocity pairs guaranteeing stability does not increase enormously in the x-y planes, there are many more peaks in the z directions (a higher concentration of red-marked points), that means a larger basing of attraction.

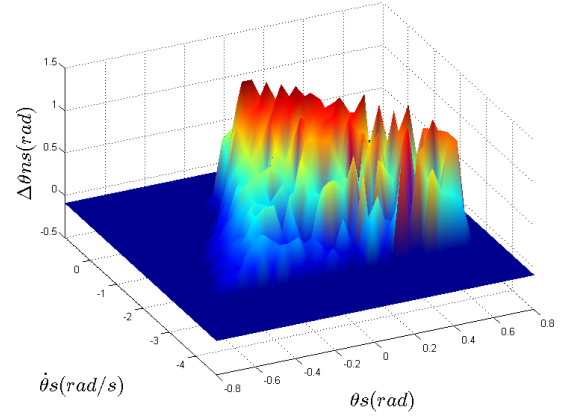


Fig. 3. Basin of Attraction Density Function:  $\theta_s \times \dot{\theta}_s \times \Delta\theta_{ns}$  - Passive

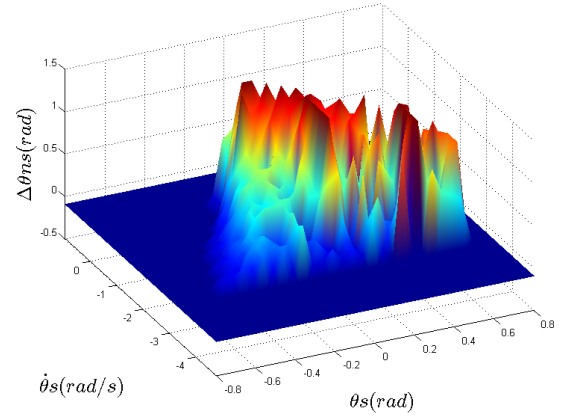


Fig. 4. Basin of Attraction Density Function:  $\theta_s \times \dot{\theta}_s \times \Delta\theta_{ns}$  - Controlled

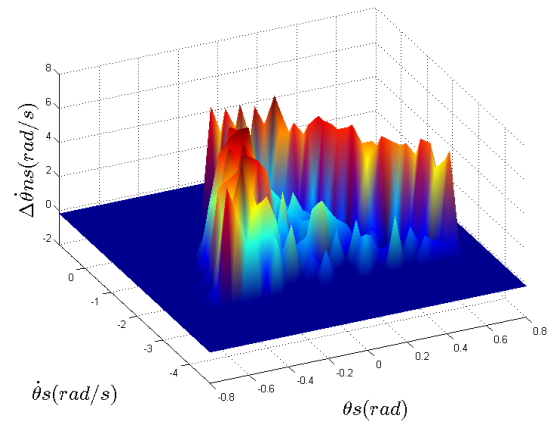


Fig. 5. Basin of Attraction Density Function:  $\theta_s \times \dot{\theta}_s \times \Delta\dot{\theta}_{ns}$  - Passive

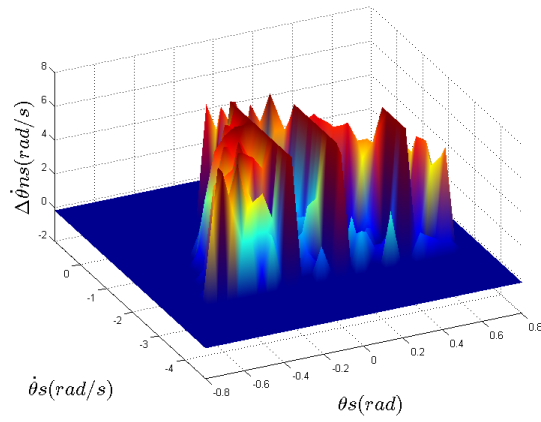


Fig. 6. Basin of Attraction Density Function:  $\theta_s \times \dot{\theta}_s \times \Delta\dot{\theta}_{ns}$  - Controlled

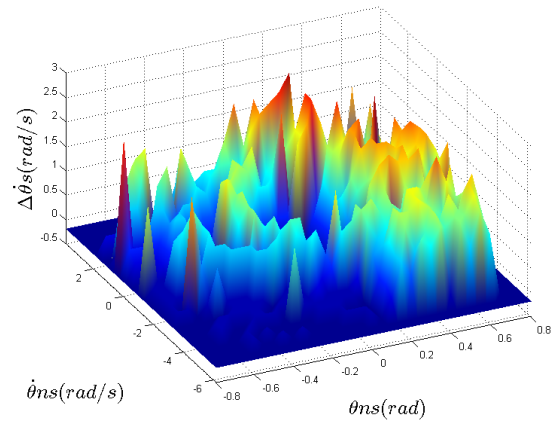


Fig. 9. Basin of Attraction Density Function:  $\theta_{ns} \times \dot{\theta}_{ns} \times \Delta\dot{\theta}_s$  - Passive

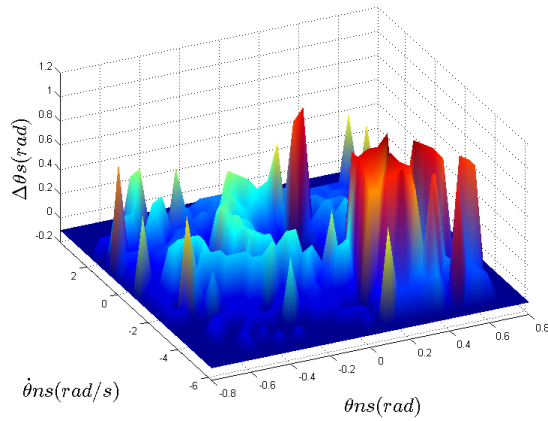


Fig. 7. Basin of Attraction Density Function:  $\theta_{ns} \times \dot{\theta}_{ns} \times \Delta\theta_s$  - Passive

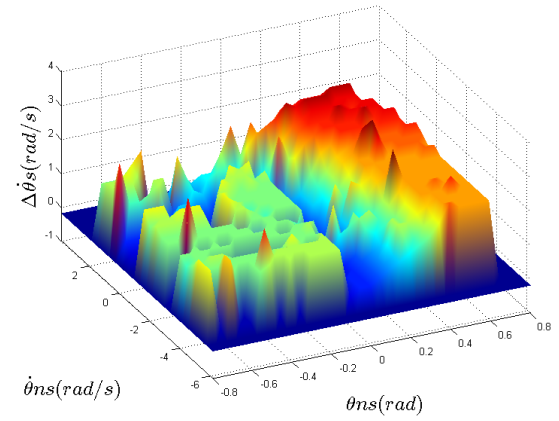


Fig. 10. Basin of Attraction Density Function:  $\theta_{ns} \times \dot{\theta}_{ns} \times \Delta\dot{\theta}_s$  - Controlled

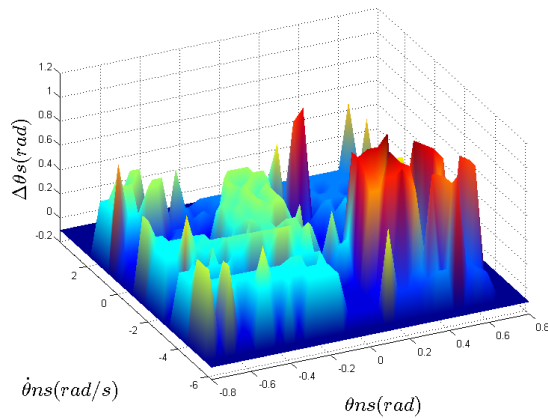


Fig. 8. Basin of Attraction Density Function:  $\theta_{ns} \times \dot{\theta}_{ns} \times \Delta\theta_s$  - Controlled

By looking at the complexity of the resulting graphs and taking into account the number of varied parameters, it indicates that the system might be further analyzed in order to extrapolate all the factors affecting the stability of the biped model. Thus, future research plans include a sensitive analysis of the inertial parameters of the model, in which the mass of the legs will be varied in relation to the hip one and a second one, where the mass of the stance leg varies with respect to that of the swing leg, thus breaking the model symmetry. The importance of the inertia distributions will be studied at that point, as well as the different dynamic behavior of the two legs.

The graphical analysis also reveals a certain difficulty in controlling the stance leg, as peaks are randomly distributed in the graph. Thus, a more accurate analysis includes an investigation of a reasonable explanation for this. An interesting result is found in the regular behavior of the swing leg. This is crucial for the execution of the subsequent step [11].

Moreover, it is also possible to analyze the influence of the variation of the dimensions of the segments in order to obtain the proportions that result in better stability (larger basin of attraction). Finally, the increase of the basin of attraction will be evaluated as a function of the control gains variation and the model will see the addition of a trunk, due to the high influence these parameters have on the system dynamics, as stated in [11].

A better understanding of the controller performance could be achieved focusing on the analysis of the switching and the control laws on a deeper level. Also, humans implement several different strategies when recovering from stumbles [12]. A better understanding of these strategies could lead to insights of how to improve the performance of the proposed control algorithm. The main addressed aspect might be the exchange of energy during the support phase: the human gait exploits a double stance support phase, while the proposed biped model only uses the stance leg to support [12]. This means that the energy is fully and alternatively exchanged between the two legs, which is not optimal for stability.

As a drawback of the proposed controller, the reference limit cycle must be known in advance. It turns to be a real constraint, since most of the terrains are uneven in reality. In order to overcome this limitation it is strictly recommended the implementation of an automatic limit cycle detector. Finally, this novel controller could be a good candidate to be implemented on a real walker due to its simplicity and low computational load.

#### IV. CONCLUSION AND FUTURE WORKS

In this paper the effectiveness of a novel controller based on switched reference partial feedback linearization was demonstrated. The proposed, designed and simulated approach deals to an approximately increase of 210% of the passive system basin of attraction. The quite low computational cost of the controller let us think that it might be easily implemented on real biped robots prototypes, with real time stability improvements.

Future works will firstly include the elaboration of new experiments and new numerical assessments to better evaluate and show the effective performances of the control scheme presented. Secondly, a sensitive analysis will be performed, by discreetly varying the values of the system point masses; this is in order to study the best weight distribution assuring stability. Finally, a trunk will be added to the physical model; thus, it will be evaluated the effect of using the switching law algorithm to control the new introduced degree of freedom.

#### REFERENCES

- [1] T. McGeer, "Passive dynamic walking," *The International Journal of Robotics Research*, vol. 9, no. 2, pp. 62–82, 1990. [Online]. Available: <http://ijr.sagepub.com/content/9/2/62.abstract>
- [2] Y. Sakagami, R. Watanabe, C. Aoyama, S. Matsunaga, N. Higaki, and K. Fujimura, "The intelligent asimo: system overview and integration," in *Intelligent Robots and Systems, 2002. IEEE/RSJ International Conference on*, vol. 3, 2002, pp. 2478 – 2483.
- [3] K. Kaneko, K. Miura, F. Kanehiro, M. Morisawa, S. Nakaoka, and S. Kajita, "Cybernetic human hrp-4c," in *Humanoid Robots, 2009. Humanoids 2009. 9th IEEE-RAS International Conference on*, December. 2009, pp. 7 –14.
- [4] M. Vukobratovic and B. Borovac, "Zero-moment point thirty five years of its life," *International Journal of Humanoid Robotics*, vol. 1, no. 1, p. 157–173, Jan. 2004.
- [5] S. Lohmeier, T. Buschmann, and H. Ulbrich, "Humanoid robot lola," in *Robotics and Automation, 2009. ICRA '09. IEEE International Conference on*, May 2009, pp. 775 – 780.
- [6] D. G. Hobbelen and M. Wisse, *Humanoid Robots, Human-like Machines*. I-Tech, 2007, ch. 14. Limit Cycle Walking, pp. 277 – 294.
- [7] M. Spong, J. Holm, and D. Lee, "Passivity-based control of bipedal locomotion," *Robotics Automation Magazine, IEEE*, vol. 14, no. 2, pp. 30 –40, june 2007.
- [8] F. Iida and R. Tedrake, "Minimalistic control of biped walking in rough terrain," *Auton. Robots*, vol. 28, no. 3, pp. 355–368, Apr. 2010. [Online]. Available: <http://dx.doi.org/10.1007/s10514-009-9174-3>
- [9] S. Kochuvila, S. Tripathi, and S. T.S.B., "Control of a compass gait biped robot based on partial feedback linearization," in *Advances in Autonomous Robotics*, ser. Lecture Notes in Computer Science, G. Herrmann, M. Studley, M. Pearson, A. Conn, C. Melhuish, M. Witkowski, J.-H. Kim, and P. Vadakkepat, Eds. Springer Berlin / Heidelberg, 2012, vol. 7429, pp. 117–127.
- [10] A. Goswami, B. Espiau, and A. Keramane, "Limit cycles in a passive compass gaitbiped and passivity-mimicking control laws," *Auton. Robots*, vol. 4, no. 3, pp. 273–286, Jul. 1997. [Online]. Available: <http://dx.doi.org/10.1023/A:1008844026298>
- [11] M. Wisse, "Essentials of dynamic walking; analysis and design of two-legged robots," 2004.
- [12] A. Forner Cordero, H. Koopman, and F. C. van der Helm, "Energy analysis of human stumbling: the limitations of recovery," *Gait & posture*, vol. 21, no. 3, pp. 243–254, 2005.